We are IntechOpen,
the world's leading publisher of
Open Access books
Built by scientists, for scientists

6,900
Open access books available

185,000
International authors and editors

200M
Downloads

Our authors are among the

154
Countries delivered to

TOP 1%
most cited scientists

12.2%
Contributors from top 500 universities

CLARIVATE ANALYTICS
BOOK CITATION INDEX
INDEXED

WEB OF SCIENCE™

Selection of our books indexed in the Book Citation Index
in Web of Science™ Core Collection (BKCI)

Interested in publishing with us?
Contact book.department@intechopen.com

Numbers displayed above are based on latest data collected.
For more information visit www.intechopen.com

Acetabular loading in rehabilitation

Hana Debevec[1], Aleš Iglič[1], Veronika Kralj-Iglič[1] and Matej Daniel[3]
[1]Laboratory of Physics, Faculty of Electrical Engineering,
University of Ljubljana, Ljubljana, Slovenia
[2]Laboratory of Clinical Biophysics, Faculty of Medicine,
University of Ljubljana Slovenia
[3]Laboratory of Biomechanics, Faculty of Mechanical Engineering,
Czech Technical University in Prague, Czech Republic

1. Introduction

Acetabular fractures are produced by high energy injuries that often cause dislocation of the fragments with gaps and steps (Olson et al., 1997). The goal of operative treatment of such fractures is to restore acetabular anatomy with perfect fragment reduction and stable fixation in order to enable early joint movement (Letournel and Judet, 1993). The fixation of the fragments is not strong enough to allow weight bearing before the bone is healed (Goulet et al., 1994; Olson, 2003) and in some patients even physical therapy with initial passive motion and continued active exercises without weight bearing could lead to dislocation of fragments and early posttraumatic osteoarthritis (Letournel and Judet, 1993).

Early physical therapy of patients with acetabular fractures therefore requires careful selection of exercises in order to prevent excessive loading of the injured acetabular region. Current guidelines for nonoperative management of acetabular fractures and postoperative management of surgical procedures in the acetabular region recommend initial bed rest followed by passive motion in the hip joint. Initial active non-weight-bearing exercises commence a few days after surgery and include active flexion, extension and abduction in the hip in the upright position. The same set of exercises in supine or side-lying abduction is usually postponed until 5-14 days postoperatively. Partial weight-bearing with stepwise progression usually starts 6 weeks postoperatively and full weight bearing is eventually allowed at 10 weeks (Maurer et al., 1997).

Recently, interesting information was obtained by direct measurements of acetabular contact pressures during rehabilitation exercises in subject with pressure-instrumented partial endoprostheses where it was found that acetabular pressures may not follow the predicted rank order corresponding to the commonly prescribed temporal order of rehabilitation activities (Givens-Heiss et al., 1992; Tackson et al., 1997). It has been found that hip stress magnitudes in some non-weight bearing exercises can exceed hip stress in weight bearing exercises or even gait.

Due to technical complexity and invasiveness of direct contact stress distribution measurement, various mathematical models for calculation of the contact stress distribution in the hip joint have been proposed (Brand, 2005; Daniel et al., 2008; Genda et al., 2001; Ipavec et al., 1999; 1995; Legal and Reinicke, 1980; Pedersen et al., 1997). Recently, a mathematical model has been developed that enables computation of the contact stress distribution at any given position of

acetabulum and also allows simulation of different body positions and variations in pelvic morphology. However, such estimation of the contact stress distribution necessarily includes determination of the hip joint reaction force magnitude/direction. Non-invasive determination of the localization of dynamic acetabular loading during gait has so far been performed by inverse Newtonian computations based on kinematic measurements of individual body segments and a muscle model (Delp et al., 1990). For slow rehabilitation exercises the loading in the hip joint at a given leg and/or body position approximates to static biomechanical equilibrium and the hip joint reaction force can then be numerically calculated by using a muscle model and a suitable optimization function without kinematic measurements (Crownishield and Brand, 1981; Pedersen et al., 1997).

It has been shown recently, that the acetabular loading is the highest in unsupported supine abduction (Kristan et al., 2007). However, the abduction may be accompanied with flexion and rotation of the hip as well. The aim of this chapter is to present a model for assessing acetabular loading in non-weight-bearing supine exercises by using a muscle model for computation of the hip joint reaction force and a previously developed mathematical model of contact hip stress distribution. Position of the leg with high acetabular loading will be identified. With this knowledge the range of motion and body position during active exercises can be suggested that would prevent excessive loading of particular acetabular regions and displacement of fracture fragments.

2. Hip joint force computation

2.1 Equilibrium equations

In mathematical modelling, the musculoskeletal system of human body is usually modelled as a system of absolutely stiff segments connected by joints and motion of the segments is realized by the muscles spanning the joints (Nigg and Herzog, 1995; Schneck, 1990; Winters, 2000; Zajac and Winters, 1990). From this point of view, the human body is perceived as a multibody mechanical system controlled by the equations of dynamic equilibrium (Rasmussen et al., 2001).

In the supine abduction, the body could be divided into two segments (Iglič et al., 1990). The first segment is the free leg which performs given exercise and the second segment is the rest of the body. In this position, the leg is loaded by its own weight $\mathbf{W}_L$, by the hip joint reaction force $\mathbf{R}$, and by the force of the muscles $\mathbf{F}$. It is taken that the origin of the hip joint reaction force $\mathbf{R}$ lies in the centre of the femoral head (Yoshida et al., 2006).

$$\mathbf{F} + \mathbf{W}_L - \mathbf{R} = 0 \tag{1}$$

The muscle force $\mathbf{F}$ acting on the free leg is the vector sum of the forces of all the muscles $\mathbf{F}_i$ that are active in the particular body position

$$\mathbf{F} = \sum_i \mathbf{F}_i \tag{2}$$

In the modelled two-segment system, it is taken that rotation of the segments occurs with respect to the axis through the centre of the femoral head. Therefore the centre of the femoral head was chosen for the origin of the coordinate system. In the anatomical position, the x-axes point medially, the y-axes point anteriorly, and the z-axis point superiorly (Fig. 1).

When performing slow exercise, inertial forces can be neglected and moment equilibrium of the free leg with respect to the center of the coordinate system can be written as

$$\mathbf{r_W} \times (\mathbf{W}_L) + \sum_i \mathbf{r}_i \times \mathbf{F}_i = 0 \tag{3}$$

where $\mathbf{r}_W$ is the radius vector from the centre of rotation (centre of the femoral head) to the centre of gravity of the free leg, $\mathbf{r}_i$ is the radius vector from the center of rotation to the attachment of given muscle at the free leg. The index i runs over all muscles that are active in particular leg position.

The weight of the leg is approximated after Clauser, 1970.

$$W_L = 0.161 \, W_B \tag{4}$$

where W_B is the body weight. In supine abduction, the weight of the leg points backward

$$\mathbf{W_L} = [0, -W_L, 0] \tag{5}$$

and position of the center of gravity in neutral position of the leg is approximated as

$$\mathbf{r}_W = [0, 0, -b] \tag{6}$$

where b is the z-coordinate of the center of the gravity of lower leg.

In a static biomechanical analysis, whole muscles are usually represented as single vectors with a certain line of action and force magnitude (Crownishield and Brand, 1981). The line of action of a muscle may be considered to go directly from the origin to the insertion site (Schneck, 1990). We can describe these points by their radius vectors: $\mathbf{r}_i$ for the proximal attachment point and $\mathbf{r}_i'$ for the distal attachment point. From the position of the muscle attachment points, the direction of the force of the muscle, given by the unit vector $\mathbf{s}_i$, is calculated.

$$\mathbf{s}_i = \frac{\mathbf{r}_i' - \mathbf{r}_i}{|\mathbf{r}_i' - \mathbf{r}_i|} \tag{7}$$

The muscle force $\mathbf{F}_i$ can be approximated as (Iglič et al., 1990):

$$\mathbf{F}_i = \sigma_i \, PCSA_i \, \mathbf{s}_i \qquad i = 1, \ldots, 9 \tag{8}$$

where $PCSA_i$ is physiological cross-sectional area of the i-th muscle, σ_i is the average tension in the i-th muscle and $\mathbf{s}_i$ is the unit vector in the direction of the the the i-th muscle.

2.2 Muscle model

The musculoskeletal geometry defining positions of proximal and distal muscle attachment points in neutral position and cross-sectional areas of the muscles is based on the work of (Delp et al., 1990). Muscles attached over a large area are divided into separate units. Hence, the model includes 27 effectively active muscles of the hip (Tab. 1).

2.3 Muscle force optimization

If all the muscles were included into equilibrium equations, the number of unknown quantities would be much higher than the number of equations. Mathematically, an infinite number of solutions would satisfy the system of equations. It means, there is more muscles than needed to perform given motion and the problem is referred as the muscle redundancy (Prilutsky and Gregor, 2000; Tsirakos et al., 1997).

It has been suggested that the optimal muscle activation can be found by minimization of the sum of muscle stresses cubed (Crownishield and Brand, 1981; Tsirakos et al., 1997). This optimization criterion is based on the experimentally determined nonlinear dependence between the muscle force and the endurance time of muscle contraction and on the idea that muscles

No	Muscle	No	Muscle
1	adductor brevis	15	gluteusminimus3
2	adductor longus	16	iliacus
3	adductor magnus 1	17	pectineus
4	adductor magnus 2	18	piriformis
5	adductor magnus 3	19	psoas
6	gemelli inf. et sup.	20	quadratus femoris
7	gluteus maximus 1	21	biceps femoris long
8	gluteus maximus 2	22	gracilis
9	gluteus maximus 3	23	sartorius
10	gluteus medius 1	24	semimebranosus
11	gluteus medius 2	25	semitendinosus
12	gluteus medius 3	26	tensor fascie latae
13	gluteus minimus 1	27	rectus femoris
14	gluteus minimus 2		

Table 1. Muscles included in the model of the hip.

are activated in a way that maximizes their endurance time (Brand et al., 1986). The optimization criterion was justified by comparison of the resultant hip force calculation with the experimental measurements using an implanted instrumented endoprosthesis (Brand et al., 1994; Stansfield et al., 2003).

The physiology of muscle requires that the muscle forces are non-compressive and do not exceed their physiological limits (Heller et al., 2001; Tsirakos et al., 1997). Therefore additional inequality constraints were defined which restrict the range of the muscle forces F_i. The maximum allowed muscle force of the i-th muscle is directly proportional to the physiological cross-sectional area (Crownishield et al., 1978) and the maximum allowed tensile stress in the muscle (σ_{max}). In our work the value of 1 MPa was taken for σ_{max} (Crownishield and Brand, 1981; Heller et al., 2001). By taking into account equilibrium of the forces and the moments acting on the pelvis in the rehabilitation exercise (Eq. (3)) and definition of muscle force using a straight-line muscle model (Eq. (8)), the optimisation problem can be defined:

$$
\begin{aligned}
\text{minimize} \quad & G = \sum_{i=1}^{N} \sigma_i^3 \\
\text{subject to} \quad & \mathbf{r_W} \times (\mathbf{W}_L) + \sum_i \mathbf{r}_i \times \mathbf{F}_i = 0 \\
& 0 \leq F_i \leq \sigma_{max} \, PCSA_i \qquad i = 1, \ldots, N
\end{aligned}
\tag{9}
$$

For solving nonlinear optimisation problems the SOLNP module for MATLAB was used. After minor adjustments of the source code, it was possible to use this module in GNU Octave as well (Eaton, 1997). The SOLNP algorithm solves the general nonlinear optimisation programming problem with an augmented Lagrangian objective function using a combination of linear programming and sequential quadratic programming using Broyden-Fletcher-Goldfarb-Shanno's technique (Ye, 1989). The further description of the algorithms used in the module SOLNP is given in Ye, 1989.

3. Hip joint contact stress distribution – HIPSTRESS model

On the basis of known values of the femoral head radius r, the geometry of the acetabulum given by the Wiberg centre-edge angle ϑ_{CE} and the angle of anteversion ϑ_{AV} (Fig. 2) and the

Fig. 1. Muscles of the hip. Cartesian coordinate system with the origin in the centre of the femoral head, xz-plane coincides with the frontal plane, xy-plane coincides with the transversal plane, x-axis points laterally, y-axis points anteriorly and z-axis points superiorly.

resultant hip force $\mathbf{R}$, the peak stress on the weight-bearing surface p_{max} can be computed by using subsequent mathematical model (Iglič et al., 2002; Zupanc et al., 2008). The original model adopts cosine stress distribution derived by (Brinckmann et al., 1981).

3.1 Cosine stress distribution

In deriving model equations, following simplifications concerning the geometry of the hip and the mechanical properties of the articular cartilage were introduced: it is assumed that the femoral head has a spherical shape while the acetabulum forms a hemisphere. The gap between these two rigid spherical surfaces is occupied by a cartilage which is considered to be an ideally elastic material, i.e., it is assumed that it obeys Hooke's law. Upon loading, the femoral head is moved toward the acetabulum and the cartilage is squeezed. Due to the assumed sphericity of the bone surfaces there is only one point where the spherical surfaces of
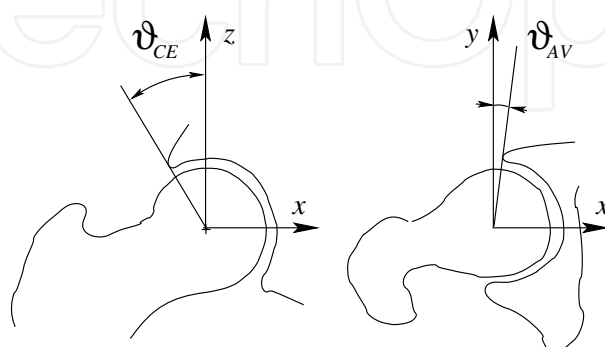

Fig. 2. Position of the acetabular cup is determined by the center-edge angle of Wiberg ϑ_{CE} and angle of anteversion ϑ_{AV}.

the acetabulum and the femur are the closest. This point is called the stress pole (Brinckmann et al., 2002). Since the cartilage completely fills the gap, the deformation of the cartilage is highest at the stress pole. From the sphericity of the bone surfaces it can be derived that the strain in the cartilage layer at any point of the weight bearing area is proportional to the cosine of the angle between this point and the stress pole (Brinckmann et al., 1981; Greenwald and O'Connor, 1971). According to Hooke's law, the contact stress in the cartilage is proportional to the strain in the cartilage, i.e., to the displacement of the femoral head with respect to the acetabulum. The sphericity of the hip surfaces and the ideal cartilage elasticity described above yield the cosine stress distribution function with its maximum at stress pole p_0 (Brinckmann et al., 1981):

$$p = p_0 \cos \nu \tag{10}$$

where ν is the angle between the given point and the stress pole. The area of nonzero contact stress is called the weight bearing area A.

3.2 Equilibrium equations

The stress distribution is described by the position of the stress pole P and value of the stress at it. The sum of the contact stresses over the weight bearing area gives the hip joint reaction force.

$$\int_A p \, \mathrm{d}\mathbf{A} = \mathbf{R} \tag{11}$$

In contrast to the previous work (Ipavec et al., 1999), we present a local coordinate system, which is fixed with respect to the acetabulum instead of global coordinates. The acetabular coordinate system is defined in accordance with Bergmann, 2001. The acetabular coordinate system takes advantage of the symmetry of the acetabular hemisphere.

The hip joint resultant force is calculated in a coordinate system which is fixed with respect to the pelvis. The position of the acetabular cup with respect to the pelvis coordinate system is determined as described in (Bergmann, 2001). The origin of the pelvis Cartesian coordinate system and of the acetabular Cartesian coordinate system coincides with the center of the femoral head. The local coordinate system of the acetabulum is obtained after rotation of the pelvis coordinate system (Bergmann, 2001) for angle β around the x axis and then by angle γ around the z axis (Fig. 3). After the rotation the acetabular xz-plane is identical with the basis of the acetabular hemisphere and the $-y$ axis points to the top of the acetabular shell. After subsequent transformation of coordinate system defined as $x_a = z$, $y_a = z$ and $z_a = -y$, a coordinate system shown in Fig. 4 is obtained. The z_a-axis is the axis of the symmetry of the acetabular hemisphere, y_a-axis points anteriorly and x_a-axis points laterally.

The values of the angles β and γ for a normal hip are computed from position of the acetabulum as:

$$\gamma = \frac{\pi}{2} - \vartheta_{AV} \tag{12}$$

$$\beta = \arctan\left(\frac{\tan(\vartheta_{CE})}{\sin(\gamma)}\right) \tag{13}$$

where ϑ_{CE} is the center-edge angle of Wiberg and ϑ_{AV} is the angle of anteversion defined in Fig. 2.

In the acetabular coordinate system, the hip joint resultant force $\mathbf{R}$ is defined by its magnitude R and by its direction, given by the spherical coordinates $\vartheta_{Ra}, \varphi_{Ra}$. The position of the stress pole is also determined by spherical coordinates Θ_a and Φ_a. The polar angles ϑ_{Ra} and
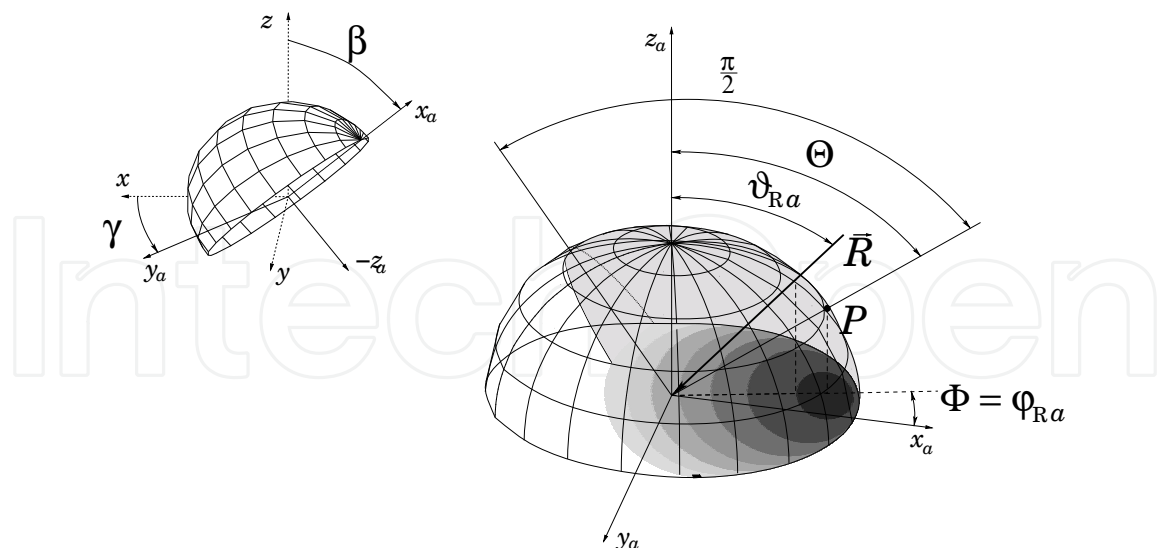
Fig. 3. Position of the acetabular coordinate system (x_a, y_a, z_a) with respect to the pelvic coordinate system (x, y, z) (Bergmann, 2001) (left) and schematic presentation of the acetabular hemisphere and the acetabular coordinate system (right). The weight bearing area is marked by shading, symbol P denotes position of the stress pole (right). The projection of the stress distribution in the xz-plane is also shown.

Θ_a describe the angular displacement from the z_a-axis, while the azimuthal angles φ_{Ra} and Φ_a describe the angular displacement of the pole from the $y = 0$ plane in counterclockwise direction.

Due to the symmetry of the acetabular coordinate system, where the z_a axis is the axis of symmetry of the acetabular shell, angle Φ_a is given by the direction of force φ_{Ra} only as discussed below. Force **R** and the z_a-axis of the acetabular coordinates determine the symmetry plane which divides the acetabular hemisphere into two equal parts. The contact stress distribution should satisfy the condition that integration of p over the area of both halves of the acetabular hemisphere (Fig. 4) gives the resultant hip force (Eq. 11). Since in our model the weight bearing is a part of the acetabular hemisphere, and the stress distribution function (Eq. (10)) is symmetrical with respect to the stress pole, Eq. (11) is fulfilled only in the case if the stress distribution is symmetrical with respect to the plane given by φ_{Ra} and y axis. It means that the stress pole must lie in this symmetry plane defined by R and the y-axis ($\Phi_a = \varphi_{Ra}$).

Using appropriate rotation of the coordinate system around the z_a-axis for angle φ_{Ra} we obtain a new orthogonal coordinate system x'_a, y'_a, z'_a. In the rotated coordinate system the pole of stress P as well as force **R** lie in the $y'_a = 0$ plane. For a force in $y'_a = 0$ plane, method for determination of the position of the stress pole which was developed for the one-leg standing with the force in the frontal plane and acetabulum symmetrical with respect to this plane (Herman et al., 2002; Iglič et al., 1993; 2002) can be used.

In order to solve Eq. (11), the ordinary spherical coordinate system was used in the previous papers (Iglič et al., 1993; Ipavec et al., 1999). Classical spherical coordinates lead to the complex expression for the boundaries of the weight-bearing area. Therefore the corresponding integrals in Eq. (11) are mathematically complicated (Ipavec et al., 1999). If the alternative spherical coordinate system is used the calculation of the integrals in vector Eq. (11) becomes much more simple and transparent (Herman et al., 2002). The alternative spherical coordi-

nates are defined as following:

$$x'_a = r \cos \varphi \sin \vartheta \tag{14}$$

$$y'_a = r \sin \varphi \tag{15}$$

$$z'_a = -r \cos \varphi \cos \vartheta \tag{16}$$

where r is the radius of the articular surface. Angles ϑ and φ are depicted in Fig. 4. In the rotated alternative coordinate system (Fig. 4) force $\mathbf{R}$ and the stress pole will have the spherical coordinates $\varphi'_{Ra} = 0$, $\vartheta'_{Ra} = \vartheta_{Ra}$ and $\Phi'_a = 0$, $\Theta'_a = \Theta_a$, respectively. In the rotated spherical coordinates the angle ν between the radius vector to the stress pole

$$\mathbf{r}_{\mathrm{P}} = (r \sin \Theta_a, 0, r \cos \Theta_a) \tag{17}$$

and the radius vector to the given point on the articular surface

$$\mathbf{r} = (r \cos \varphi \sin \vartheta, r \sin \varphi, r \cos \varphi \cos \vartheta) \tag{18}$$

can be expressed using the scalar product of $\mathbf{r}_{\mathrm{P}}$ and $\mathbf{r}$:

$$\cos \nu = \frac{\mathbf{r} \cdot \mathbf{r}_{\mathrm{P}}}{r^2} = \cos \varphi \cos \vartheta \cos \Theta_a + \cos \varphi \sin \vartheta \sin \Theta_a \tag{19}$$

Then the stress distribution function (Eq. 10) is expressed in the alternative coordinate system with the pole in the $x'_a = 0$ plane, as follows

$$p = p_0 (\cos \varphi \cos \vartheta \cos \Theta_a + \cos \varphi \sin \vartheta \sin \Theta_a) \tag{20}$$

The elementary infinitesimal integration area in the alternative coordinate system is:

$$\mathrm{d}\mathbf{A} = r^2 \cos \varphi (\cos \varphi \sin \vartheta, \sin \varphi, \cos \varphi \cos \vartheta) \, \mathrm{d}\vartheta \, \mathrm{d}\varphi \tag{21}$$

In the new alternative coordinate system, the integration in Eq. (11) can be performed over the fixed boundaries of the weight-bearing area, which considerably simplifies the derivation. The weight bearing area is limited at the lateral border by the acetabular rim ($\vartheta_L = \pi/2$, while the medial border is determined by the curve where the stress vanishes (Eq. 10), i.e., the lateral border consists of points with a constant angular distance $\pi/2$ from the stress pole ($\vartheta_M = \Theta_a - \pi/2$). Since the symmetry plane defined by force $\mathbf{R}$ and the y-axis splits the acetabular hemisphere into two symmetrical parts (Fig. 4), in the new alternative coordinate system angle φ runs from $-\pi/2$ to $\pi/2$ over the whole weight-bearing area.

It follows from Eqs. (20) and (21) that the x'_a and z'_a components of force $\mathbf{R}$ in Eq. (11) can be expressed in the form:

$$R \cos \vartheta_{Ra} = p_0 r^2 \int_{\vartheta_M}^{\vartheta_L} \cos \vartheta \cos(\vartheta - \Theta_a) \, \mathrm{d}\vartheta \int_{-\frac{\pi}{2}}^{\frac{\pi}{2}} p \, \cos^3 \varphi \, \mathrm{d}\varphi \tag{22}$$

$$R \sin \vartheta_{Ra} = p_0 r^2 \int_{\vartheta_M}^{\vartheta_L} \sin \vartheta \cos(\vartheta - \Theta_a) \, \mathrm{d}\vartheta \int_{-\frac{\pi}{2}}^{\frac{\pi}{2}} p \, \cos^3 \varphi \, \mathrm{d}\varphi \tag{23}$$

The integral for the x'_a component of force $\mathbf{R}$ is identically equal to zero due to the symmetry of the rotated coordinate system as discussed above (Fig. 4).
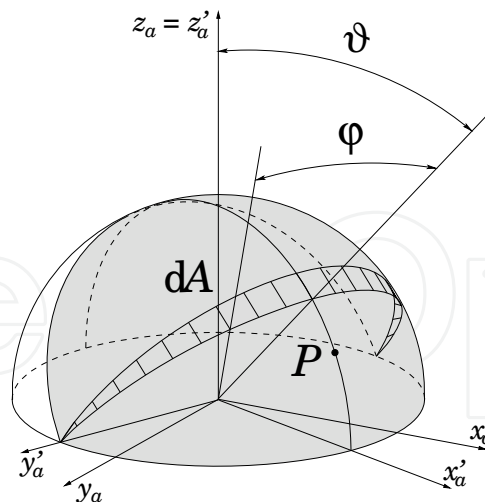
Fig. 4. Rotated acetabular coordinate system (x'_a, y'_a, z'_a) and the alternative spherical coordinate system in the acetabular reference frame. Weight-bearing area is shaded and the elementary area dA is shown. Symbol P denotes the position of the stress pole.

It follows from Eqs. (22) and (23) that the unknown spherical coordinate of the stress pole (Θ_a) can be obtained by solving the nonlinear equation:

$$\tan(\vartheta_{Ra} + \Theta_a) = \frac{\sin^2 \Theta_a}{\pi - \Theta_a + \sin \Theta_a \cos \Theta_a} \tag{24}$$

When the position of the stress pole (Θ_a, Φ_a) is calculated as described above, the value of the stress at the pole is then determined from the expression:

$$p_0 = \frac{3\,R\,\cos(\vartheta_{Ra} + \Theta_a)}{2\,r^2\,(\pi - \Theta_a + \sin \Theta_a \cos \Theta_a)} \tag{25}$$

If the pole of the stress distribution is located within the weight-bearing surface, the location of the p_{max} coincides with the location of the pole (p_{max} equals p_0). When the stress pole lies outside the weight-bearing surface, the stress is maximal at the point on the weight-bearing surface, which is closest to the pole and can be computed after Eq. (10).

4. Modelling rehabilitation exercises

Each specific type of exercise was modeled by rotation of the leg around the center of the femoral head while the pelvis was taken to be fixed in a laboratory coordinate system. Three subsequent rotations were considered: abduction, flexion and internal/external rotation. Abduction angle is defined as rotation of the leg around y-axis, flexion angle is defined as rotation of the leg around x-axis and internal/external rotation is defined as rotation of the leg around z-axis (Fig. 5). Positive values of abduction angle indicate abduction while negative values indicate adduction. Positive values of flexion angle correspond to flexion while negative values correspond to extension. Positive values of rotation angle correspond to external rotation while negative values correspond to internal rotation. The three anatomic angles giving the three rotations corresponds to Euler angles (Kreyszig, 1993). Using these three angles any rotation may be described according to Euler's rotation theorem. For a given set of rotation
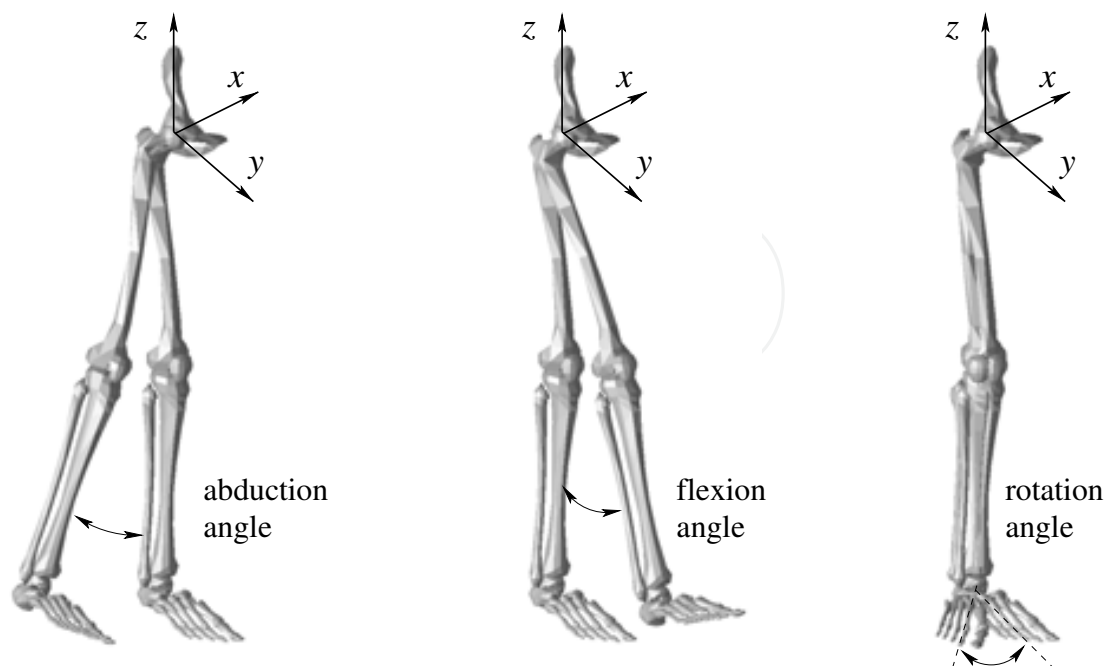
Fig. 5. Angles defining position of the leg with respect to the hip rotation. Positive directions of the angles are depicted.
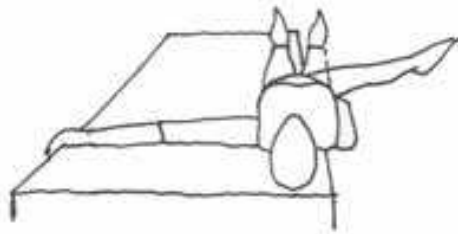

Fig. 6. Unsupported supine exercise.

angles (Fig. 5), the muscle geometry was adapted considering change in the attachment points of muscles on the bones of the leg.

5. Parameters and constants

The range of abduction/adduction was taken from 40 to -10 degrees, respectively, the range of flexion/extension was taken from 70 to -10 degress, respectively and the range of internal/external rotation was taken from -20 to 20 degress, respectively. The z-coordinate of the center of gravity of the leg b was taken to be 42.3 cm. Body weight W_B was taken to be 800 N. Position of acetabulum was defined by angles $\vartheta_{CE} = 30°$ and $\vartheta_{AV} = 15°$. Radius of articular surface r was taken to be 2.5 cm.

Rotation angle = 0 deg

Rotation angle = 20 deg

Rotation angle = −20 deg
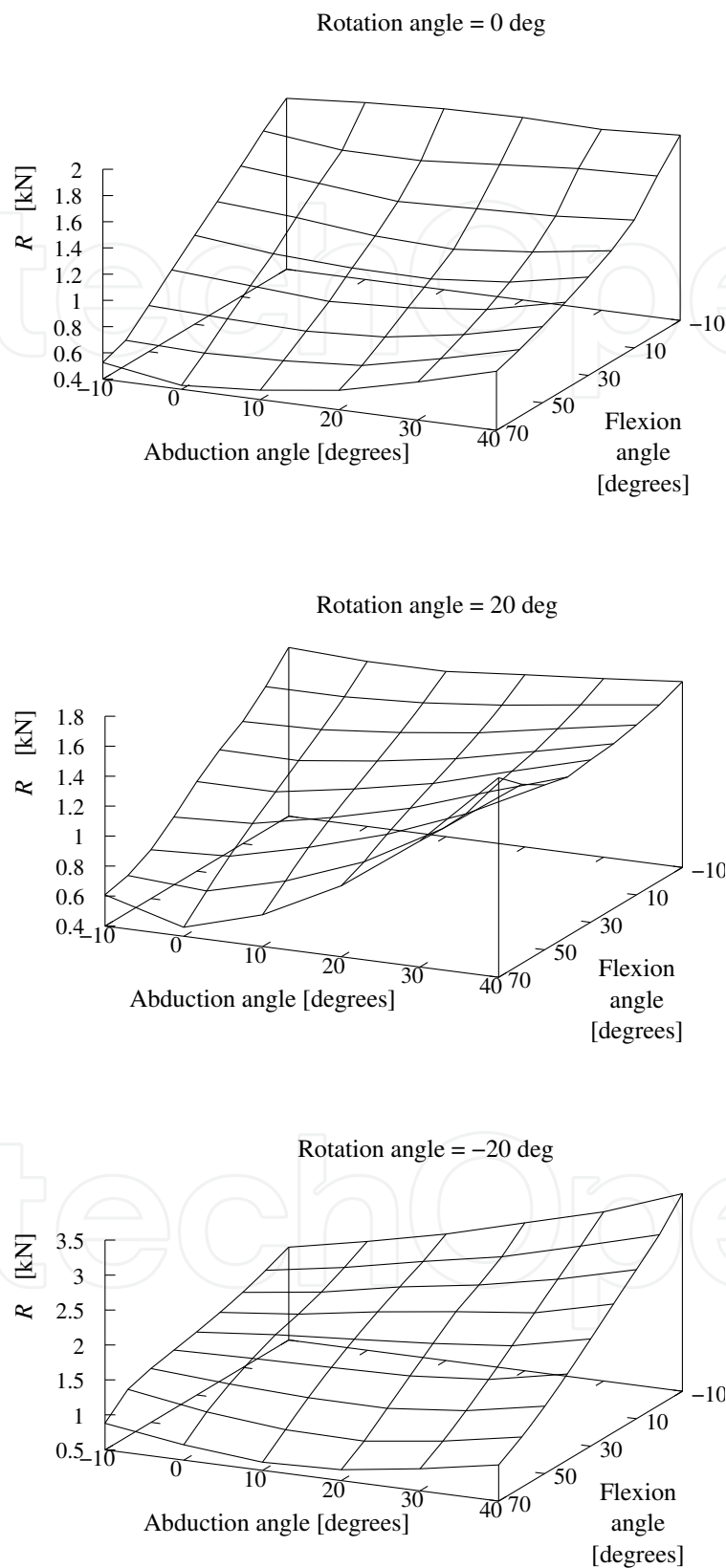
Fig. 7. Magnitude of the hip joint force R in the hip joint for various positions of the leg during supine exercises. No knee flexion is assumed.

Rotation angle = 0 deg
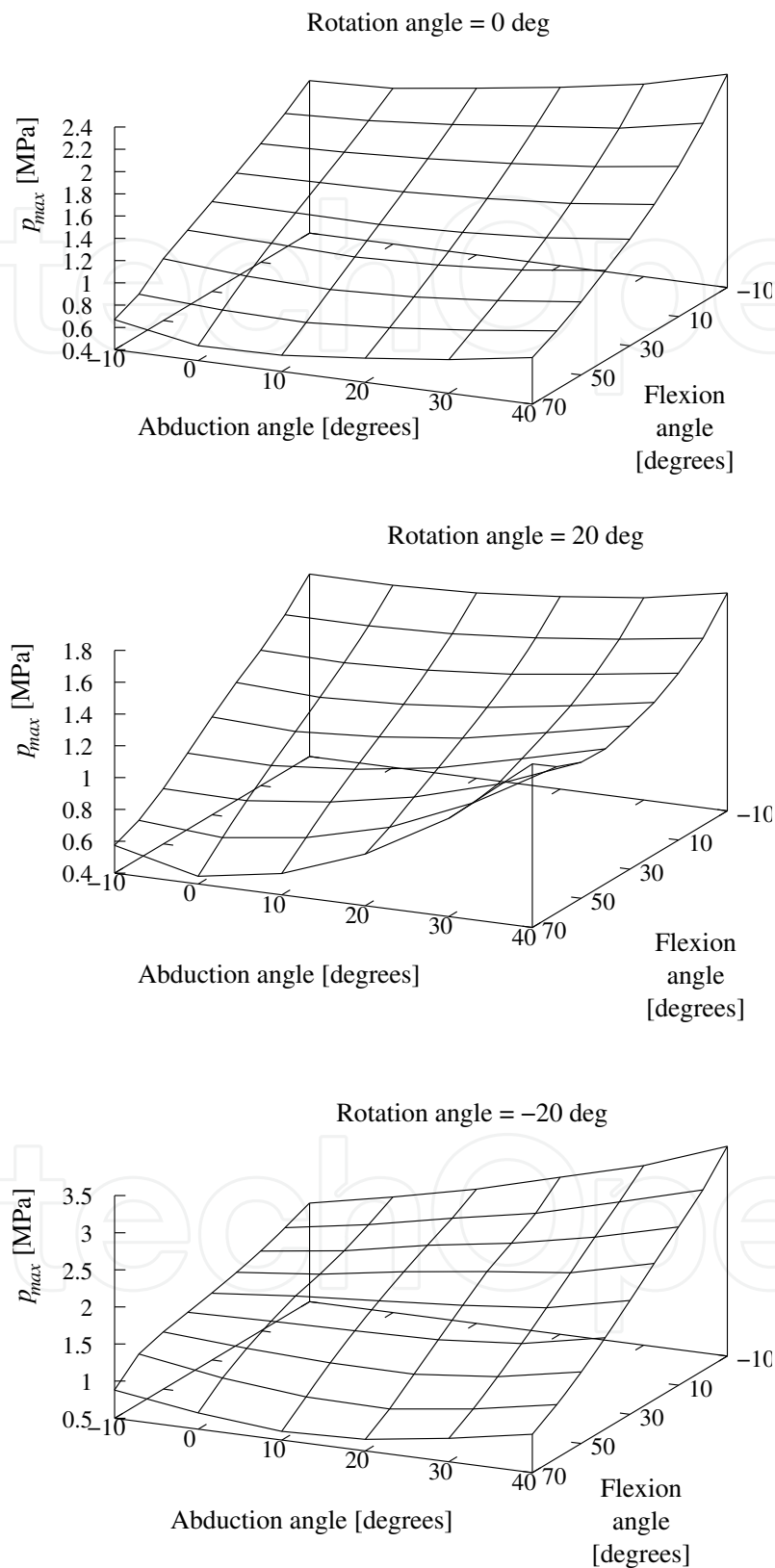
Rotation angle = 20 deg

Rotation angle = −20 deg

Fig. 8. Peak contact stress p_{max} in the hip joint for various positions of the leg during supine exercises. No knee flexion is assumed.
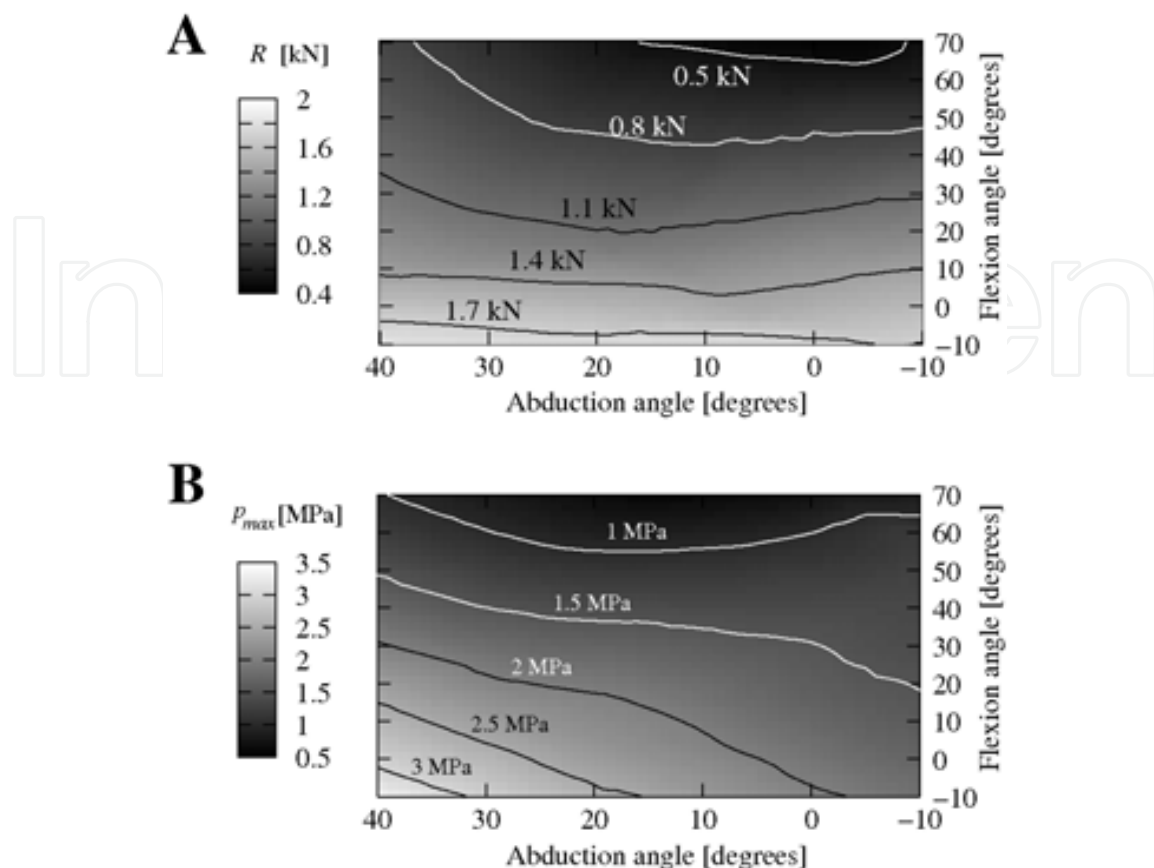
Fig. 9. (A) Magnitude of the hip joint force R and (B) peak contact stress p_{max} in the hip joint for various positions of the leg during supine exercises. No knee flexion is assumed and angle of rotation is taken to be -20 degrees.

6. Results

Previous study shows that the highest acetabular loading was observed in unsupported supine abduction (Kristan et al., 2007) (Fig. 6). Therefore, we have tested the effect of straight-leg exercise about the hip on the hip joint resultant force R and peak contact stress p_{max}.
The magnitudes of the hip joint reaction force **R** and the peak contact stress p_{max} during various positions in rehabilitation exercises in supine body positions are shown in Fig. 7 and Fig. 8 respectively. Fig. 9 shows overview of forces and stresses for rotation angle -20 degrees. Flexion in the hip has greater effect on the resulting loading of the acetabulum than the abduction. The hip joint reaction force R as well as the peak contact hip stress p_{max} is the highest in the unsupported supine extension of the hip. The hip joint loading is the lowest in hip flexion.

7. Discussion

In aggreement with previous studies (Kristan et al., 2007; Tackson et al., 1997), we have found that in the neutral leg position the hip joint reaction force is high for unsupported supine body position. This can be explained by considering the equilibrium of the moments of the gravitational and muscular forces with respect to the center of rotation of the hip joint in different leg positions. In the unsupported supine abduction, the leg has a tendency to extend and hence

the activity of flexors is required. In the supine abduction flexors that are required to maintain this posture have smaller moment arms and thus demand high flexor forces. Therefore the hip joint reaction force magnitude in unsupported supine position is considerably high. Flexion about the hip decreases the moment arm of the weight of the leg and hence decreases loading. Extension of the hip decreases the effective arms of the flexors and it increase the required muscle force as well as the hip joint reaction force.

Computed values of hip joint reaction force and peak contact hip stress reported in this study are of the same order of magnitude as the ones performed in non-weight-bearing exercises measured in vivo (Givens-Heiss et al., 1992; Tackson et al., 1997). Direct measurements of peak contact stress in supine body positions were found to be 2.8 MPa and 3.8 MPa in vivo (Givens-Heiss et al., 1992; Tackson et al., 1997) versus 3.5 MPa in our study. The reports do not specifically mention the amount of vertical leg support in supine adduction, but considering the fast velocities it could be inferred that the abduction was unsupported. It should be noted, however, that these in vivo measurements were performed with angular velocities above $30°$ and therefore also include the dynamic component of loading.

The limitations of the direct stress measurement method (Morrell et al., 2005) include the facts that the sensors measure the cartilage-on-metal surface and not the cartilage-on-cartilage surface, that the metal prosthesis in contact with natural acetabulum may differ from physiologic morphology of the hip, that sensors were located on the femoral head surface while the values of stress on the acetabular joint surface were estimated from the kinematic data. Further, hip pressure measurements of abduction exercises were performed in one patient only.

On the other hand, our method is limited by the model assumptions. In the calculation of the acetabular loading, it was assumed that the pelvis is fixed. Small rotations of the pelvis are not likely to influence the hip joint reaction force. However, if the rotations of the pelvis were large, this would represent a significant limitation of the study. The muscles were considered as active springs which are able to generate force in order to maintain body position. The passive forces generated by the muscle-tendon unit were not taken into account. To better describe the properties of the muscle, a forward dynamics optimization including activation dynamics and musculo-tendon contraction dynamics could be used Thelen et al. (2003). The static optimization method used in this study to compute muscle forces cannot predict muscle co-contraction Tsirakos et al. (1997). To improve the description of the muscle forces during exercises, a dynamic optimization approach that takes into account dynamic properties of neuromusculoskeletal system could be used. Also, within the static approaches, there are differences according to the choice of the optimization criterion Prilutsky and Gregor (2000). However, comparison of measurements and calculations of the hip joint reaction force showed that the type of the optimization criterion employed does not significantly influence the calculated hip joint reaction force.

In the mathematical model of hip stress calculation, several simplifications were used that could influence the accuracy of the calculated contact stress distribution. For example, in our model the femoral head and acetabulum are taken to be spherical. In normal hips the femoral head and the acetabulum are actually out-of-round by 1-3 mm. It has be shown that in the case of an ellipsoidal articular surface with the semiaxes r and $r + \triangle r$, the cosine stress distribution function (Eq. (10)) can be modified by taking into account the perturbation of the first order in $\triangle r / r$ which yields the stress distribution function in the form $p = p_0 \cos \gamma (1 + 3(\triangle r / r) \sin^2 \gamma)$ (Ipavec et al., 1997). Our mathematical model derivation also assumes that the cartilage layer has constant thickness and mechanical properties. The contact stress was assumed to be proportional to the cartilage deformation δ. If the properties of the cartilage

vary along the articular surface, the contact stress at a given point also varies, and this is not taken into account in our model.

The mechanics of cartilage layer in the hip joint obviously cannot be fully described as a homogeneous continuum and a linear elastic material. In order to approach a more realistic description of the stress and force distribution in the cartilage layer, one should take into account the specific molecular structure of the joint articular surface where the two glycoprotein monolayers are adsorbed on the cartilage of both contact surfaces (Nordin and Frankel, 1989). The mechanics of this structure could be realistically described only by using the methods of theoretical physics on the molecular level developed in the field of polymer physics and the statistical physics of interfaces.

We have assumed hip exercises with straight leg only, i.e. no knee flexion was assumed. This assumtion is not fully realistic as the hip flexion is usually acompanied with the flexion in the knee. Also the range of motion in the hip may considerably change if the knee flexion is assumed (Čihák, 2002).

The accuracy of the acetabular loading predicted in this paper could be certainly improved by removing some of the above mentioned simplifications assumed in our mathematical model. However, we believe that the main conclusions would not be changed by using a more advanced mathematical model.

8. Conclusions and further research

We conclude that absolute values of the hip joint reaction force and the peak contact hip stress in unsupported supine abduction are the highest in combination of hip extension, hip abduction and internal rotation. The stresses and force can reach the values observed in weight-bearing exercises or gait (Ipavec et al., 1999). Unsupported Supine abduction in initial rehabilitation phases should be therefore omitted or recommended with ground support (on the bed) or in combination with assisted flexion.

Based on the presented results we suggest that detailed calculations of spatial distribution of the hip joint contact stress is required before starting rehabilitation procedure as to individually design the rehabilitation procedure for a given patient. In the planning, the spatial position of the fracture lines and dislocations of the acetabular fragments should be taken into account.

Our results complement the results of direct measurements of stress during exercises and the experience – based exercise protocols in elucidating the mechanical impacts on the rehabilitation. In further work, stress distributions in other body positions should computed as well in order to select an appropriate therapy for given patient.

9. References

Afoke, N., Byers, P., and Hutton, W. (1987). Contact pressures in the human hip joint. *Journal of Bone and Joint Surgery*, 69B(4):536–541.

Bergmann, G. (2001). *Hip98, Loading of the hip joint.* Freie Universität, Berlin. available online at ftp://ftp.ukbf.fu-berlin.de/pub/biomech/hip98.zip.

Brand, R. (2005). Joint contact stresses: A reasonable surrogate for biological processes? *The Iowa Orthopaedic Journal*, 25:82–94.

Brand, R., Pedersen, D., Davy, D., Kotzar, K., Heiple, K., and Goldberg, V. (1994). Comparison of the hip joint reaction force and measurements in the same patient. *Journal of Arthroplasty*, 9(1):45–51.

Brand, R., Pedersen, D., and Friederich, J. (1986). The sensitivity of muscle force predictions to changes in physiologic cross-sectional area. *Journal of Biomechanics*, 19:589–596.

Brinckmann, P., Frobin, W., and Hierholzer, E. (1981). Stress on the articular surface of the hip joint in healthy adults and persons with idiopathic osteoarthrosis of the hip joint. *Journal of Biomechanics*, 14(3):149–153.

Brinckmann, P., Frobin, W., and Leivseth, G. (2002). *Musculoskeletal biomechanics*. Georg Thieme Verlag, Stuttgart.

Brown, T. (1983). In vitro contact stress distributions in the natural human hip. *Journal of Biomechanics*, 16(6):373–384.

Clauser, C., McConville, J., and Young, J. (1970). Weight, volume and center of the mass of the human body. Technical Report Report AMRL-TR-69-70, National Technical Information Service.

Crownishield, R. and Brand, R. (1981). A physiologically based criterion for muscle force prediction and locomotion. *Journal of Biomechanics*, 14:793–801.

Crownishield, R., Johnston, R., Andrews, J., and Brand, R. (1978). A biomechanical investigation of the human hip. *Journal of Biomechanics*, 11:75–85.

Daniel, M., Iglic, A., and Kralj-Iglic, V. (2008). Hip contact stress during normal and staircase walking: the influence of acetabular anteversion angle and lateral coverage of the acetabulum. *J Appl Biomech*, 24(1):88–93.

Delp, S., Loan, J., Hoy, M., Zajac, F., Topp, E., and Rosen, J. (1990). An interactive graphics-based model of the lower extremity to study orthopaedic surgical procedures. *IEEE Transactions on Biomedical Engineering*, 37:757–767.

Eaton, J. (1997). *GNU Octave Manual*. Network Theory Ltd, Bristol, UK.

Genda, E., Iwasaki, N., Li, G., MacWiliams, B., Barrance, P., and Chao, E. (2001). Normal hip joint contact pressure distribution in single-leg standing – effect of gender and anatomic parameters. *Journal of Biomechanics*, 34:895–905.

Givens-Heiss, D. L., Krebs, D. E., Riley, P. O., Strickland, E. M., Fares, M., Hodge, W. A., and Mann, R. W. (1992). In vivo acetabular contact pressures during rehabilitation, part ii: Postacute phase. *Phys Ther*, 72(10):700–5; discussion 706–10.

Goulet, J. A., Rouleau, J. P., Mason, D. J., and Goldstein, S. A. (1994). Comminuted fractures of the posterior wall of the acetabulum. a biomechanical evaluation of fixation methods. *J Bone Joint Surg Am*, 76(10):1457–1463.

Greenwald, A. and O'Connor, J. (1971). The transmission of load through human hip joint. *Journal of Biomechanics*, 4:507–528.

Heller, M., Bergmann, G., Deuretzbacher, G., Dürselen, L., Pohl, M., Claes, L., Haas, N., and Duda, G. (2001). Musculo-skeletal loading conditions at hip during walking and stair climbing. *Journal of Biomechanics*, 34:883–893.

Herman, S., Jaklič, A., Herman, S., Iglič, A., and Kralj-Iglič, V. (2002). Hip stress reduction after Chiari osteotomy. *Medical and Biological Engineering and Computing*, 40:369–375.

Iglič, A., Kralj-Iglič, V., Antolič, V., Srakar, F., and Stanič, U. (1993). Effect of the periacetabular osteotomy on the stress on the human hip joint articular surface. *IEEE Transaction on rehabilitation*, 1(4):207–212.

Iglič, A., Kralj-Iglič, V., Daniel, M., and Maček-Lebar, A. (2002). Computer determination of contact stress distribution and the size of the weight-bearing area in the human hip joint. *Computer Methods in Biomechanics and Biomedical Engineering*, 5:185–192.

Iglič, A., Srakar, F., Antolič, V., Kralj-Iglič, V., and Batagelj, V. (1990). Mathematical analysis of Chiari osteotomy. *Acta Orthopedica Iugoslavica*, 20:35–39.

Ipavec, M., Brand, R., Pedersen, D., Mavčič, B., Kralj-Iglič, V., and Iglič, A. (1999). Mathematical modelling of stress in the hip during gait. *Journal of Biomechanics*, 32:1229–1235.

Ipavec, M., Iglič, A., Kralj-Iglič, V., and Antolič, V. (1997). Influence of the nonspherical shape of the femoral head on the compressive stress in the hip joint articular layer. In *Proceedings of the 6th Conference of Slovenian IEEE Section*, pages 351–354, Ljubljana.

Ipavec, M., Kralj-Iglič, V., and Iglič, A. (1995). Stress in the hip joint articular surface during gait. *Engineering Modelling*, 8:7–14.

Kreyszig, E. (1993). *Advanced engineering mathematics*. John Willey & Sons, New York.

Kristan, A., Mavcic, B., Cimerman, M., Iglis, A., Tonin, M., Slivnik, T., Kralj-Iglic, V., and Daniel, M. (2007). Acetabular loading in active abduction. *IEEE Trans Neural Syst Rehabil Eng*, 15(2):252–257.

Legal, H. and Reinicke, M. (1980). Zur biostatischen analyse des hüftgelenkes III. *Zeitschrift für Orthopädie und ihre Grenzgebiete*, 118:804–815.

Letournel, E. and Judet, R. (1993). *Fracture of acetabulum*. Springer, New York.

Maurer, F., Mutter, B., Weise, K., and Belzl, H. (1997). [rehabilitation following hip fractures]. *Orthopade*, 26(4):368–374.

Morrell, K. C., Hodge, W. A., Krebs, D. E., and Mann, R. W. (2005). Corroboration of in vivo cartilage pressures with implications for synovial joint tribology and osteoarthritis causation. *Proc Natl Acad Sci U S A*, 102(41):14819–14824.

Nigg, B. and Herzog, W. (1995). *Biomechanics of the musculo-skeletal system*. John Willey & Sons, Chichester.

Nordin, M. and Frankel, V., editors (1989). *Basic biomechanics of the musculoskeletal system*. Lea & Fibiger, Philadelphia.

Olson, S. A. (2003). Biomechanics of acetabular fractures. In Marvin Tile, David Helfet, J. K., editor, *Fractures of the Pelvis and Acetabulum*, pages 46–49. Lippincott Williams & Wilkins.

Olson, S. A., Bay, B. K., and Hamel, A. (1997). Biomechanics of the hip joint and the effects of fracture of the acetabulum. *Clin Orthop Relat Res*, 339(339):92–104.

Pedersen, D., Brand, R., and Davy, D. (1997). Pelvic muscle and acetabular forces during gait. *Journal of Biomechanics*, 30:959–965.

Prilutsky, B. and Gregor, R. (2000). Analysis of muscle cordination strategies in cycling. *IEEE Transactions on Rehabilitation Engineering*, 8(3):362–370.

Rasmussen, J., Damsgaard, M., and Voigt, M. (2001). Muscle recruitment by the min/max criterion - a comparative numerical study. *Journal of Biomechanics*, 34:409–415.

Schneck, D. (1990). *Engineering principles of physiologic function*. New York University Press, New York.

Stansfield, B., Nicol, A., Paul, J., Kelly, I., Graichen, F., and Bergmann, G. (2003). Direct comparison of calculated hip joint contact forces with those measured using instrumented implants. an evaluation of the three-dimensional model of the lower limb. *Journal of Biomechanics*, 26:929–936.

Tackson, S., D.E., K., and Harris, B. (1997). Acetabular pressures during hip arthritis exercises. *Arthritis Care Research*, 10(5):308–319.

Thelen, D., Anderson, F., and Delp, S. (2003). Generating dynamic simulations of movement using computed muscle control. *Journal of Biomechanics*, 36:321–328.

Tsirakos, D., Baltzopoulos, V., and Bralett, R. (1997). Inverse optimization: functional and physiological considerations related to the force sharing problem. *Critical Reviews in Biomedical Engineering*, 25(4&5):371–407.

Čihák, R. (2002). *Anatomie 1*. Grada, 2nd edition.

Winters, J. (2000). Terminology and foundations of movement science. In Winters, J. and Crago, P., editors, *Biomechanics and Neural Control of Posture and Movement*. Springer-Verlang, New York.

Ye, Y. (1989). *SOLNP user's guide: A nonlinear optimization in MATLAB*. Department of Management Sciences, College of Bussoness Administration, University of Iowa.

Yoshida, H., Faust, A., Wilckens, J., Kitagawa, M., Fetto, J., and Chao, E. Y.-S. (2006). Three-dimensional dynamic hip contact area and pressure distribution during activities of daily living. *Journal of Biomechanics*, 39:1996–2004.

Zajac, E. and Winters, J. (1990). Modelling muskuloskeletal movement systems: Joint and body segmental dynamics, muskuloskeletal and neuromuskular system. In Winters, J. and Woo, S. L.-Y., editors, *Multiple Muscle Systems - Biomechanics and Movement Organization*. Spinger-Verlang, New-York.

Zupanc, O., Krizancic, M., Daniel, M., Mavcic, B., Antolic, V., Iglic, A., and Kralj-Iglic, V. (2008). Shear stress in epiphyseal growth plate is a risk factor for slipped capital femoral epiphysis. *J Pediatr Orthop*, 28(4):444–451.
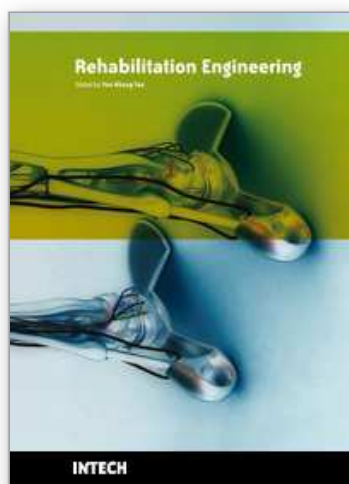
Rehabilitation Engineering

Edited by Tan Yen Kheng

ISBN 978-953-307-023-0

Hard cover, 288 pages

Publisher InTech

Published online 01, December, 2009

Published in print edition December, 2009

Population ageing has major consequences and implications in all areas of our daily life as well as other important aspects, such as economic growth, savings, investment and consumption, labour markets, pensions, property and care from one generation to another. Additionally, health and related care, family composition and life-style, housing and migration are also affected. Given the rapid increase in the aging of the population and the further increase that is expected in the coming years, an important problem that has to be faced is the corresponding increase in chronic illness, disabilities, and loss of functional independence endemic to the elderly (WHO 2008). For this reason, novel methods of rehabilitation and care management are urgently needed. This book covers many rehabilitation support systems and robots developed for upper limbs, lower limbs as well as visually impaired condition. Other than upper limbs, the lower limb research works are also discussed like motorized foot rest for electric powered wheelchair and standing assistance device.

INTECH

open science | open minds